











According to CFD results, the optimum hull geometry was found, and therefore the UV with  $n=2$  and  $\alpha=20$  is the best shape; This optimum shape is named **UV-LAHN**.

### 4.2 Optimum UV-LAHN Investigation

#### 4.2.1 Drag Coefficient

Table 3 shows the validation of the drag coefficient by experimental results. Drag values for the UV-LAHN model at Reynold number of  $2,3.10^7$  was calculated through CFD code and compared to experimental works. According to this results we note that the  $Cd$  obtained during this simulation is in good agreement with that of experimental, in the same context one can note a difference between the present study and that of White [19], Baker [20] and Karim [1]. This is due to the mesh choice as well as the closure model used in this case.

Table 3. Drag G

	Cd Exp White, N.M, 1977	Cd Baker, C, 2004	Cd MM. Karim and al, 2008	Cd Present study
Re = $2,30 \times 10^7$	0,00123 $\pm 0.000314$	0.00167	0.00104	0.00108

#### 4.2.2 Velocity Profile

The figure 10 shows the variation of the flow velocity through  $xy$  plan. The evolution of the boundary layer along the walls of the computational domain has been well predicted. In addition, the wake development downstream of the UV has been correctly captured.

One can also note that the realistic prediction of the acceleration of the fluid at the reduced sections between UV and the walls of the domain.

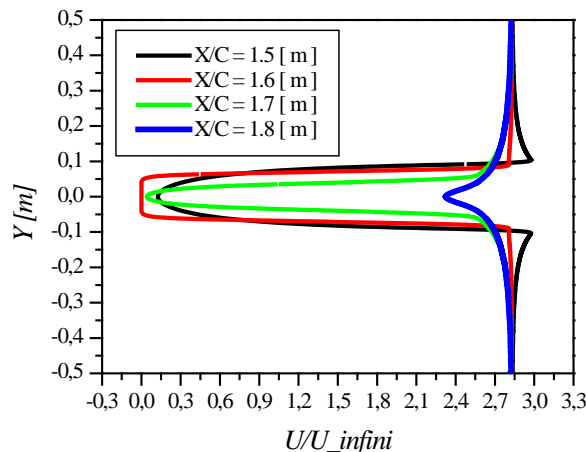


Fig.11: Velocity profil in XY plane

#### 4.2.3 Added Mass and Damping Force

The added mass is a movement effect of the water on the UV. Therefore, the effect of viscosity can be considered as two separate factors. The first one is the skin friction which is caused by viscosity shear force of a fluid flowing along the hull, and the other is the form drag caused by development of a boundary layer and the resulting difference of pressure distribution between front and stern of the vehicle.

Table 4. Add mass formulation

DOF	MOTION DESCRIPTION	EQUATION
1	Surge (Motions in the x-direction)	$\lambda_{11}=F_x/A_x$ (9)
2	Sway (Motions in the y-direction)	$\lambda_{22}=F_y/A_y$ (10)
3	Yaw (Rotations in the z-direction)	$\lambda_{26}=M_y/A_y$ (11)

The figure 11 shows the variation of UV-LAHN for the added masses  $\lambda_{11}$ ,  $\lambda_{22}$ ,  $\lambda_{26}$  immersed in water Reynold number.

The added mass of the three components, calculated using ANSYS CFX, perfectly reflects the effect of translation and rotation in the three directions.

An inverse relationship between the coefficients of the added mass and the acceleration is noted, i.e. an increase in acceleration causes a decrease in coefficients of added mass (eq 9, 10, 11).

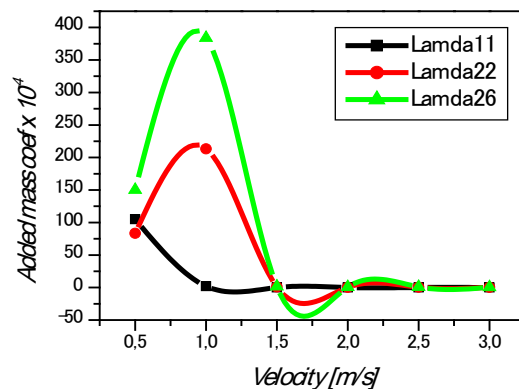


Fig.12: Added mass coefficients

The damping forces and moments act on any moving body in a supposed viscous fluid. They are due to the action of the added mass of water and the viscous friction of the fluid on the moving body. Assuming that the vehicle rotates uniformly around the specified center, the distance between vehicle centroid and circular motion center is given by R,

hence the hydrodynamic forces can be formulated as follows [11]:

$$qSC_{y1}(\alpha) + qSC_{y1}(\omega_{z1}) \approx qSC_{y1}^{\alpha} \alpha + qSC_{y1}^{\omega_{z1}} \omega_{z1} = \quad (12)$$

$$N + \lambda_{11} V \omega_{z1} \cos \alpha$$

$$qSlm_{z1}(\alpha) + qSlm_{z1}(\omega_{z1}) \approx qSlc_{m_{z1}}^{\alpha} \alpha + qSlc_{m_{z1}}^{\omega_{z1}} \omega_{z1} = \quad (13)$$

$$M + \lambda_{26} V \omega_{z1} \cos \alpha + (\lambda_{22} - \lambda_{11}) V^2 \sin \alpha \cos \alpha$$

Where the notation  $N$  and  $M$  are the normal force and pitch moment, the rotating  $\omega_{z1}$  is the angular speed, the velocity at vehicle centroid will be  $V = R\omega_{z1}$ , the damping force coefficient is  $C_{y1}^{\omega_{z1}}$  and the pitch damping moment coefficient is  $C_{m_{z1}}^{\omega_{z1}}$ .

Figure 12 show the hydrodynamic force with the increase depends on the velocity increasing. The figure shows a logical result comparing with the work of Chin [21].

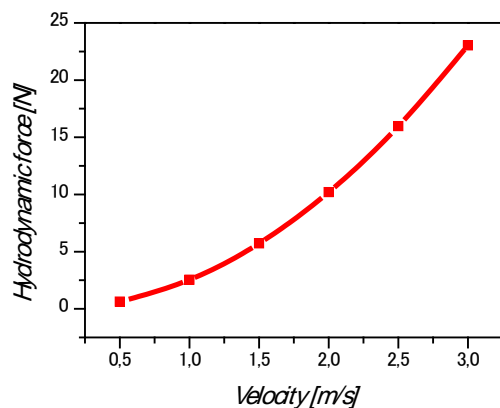


Fig.13: Hydrodynamic damping force

## 5 Conclusion

This article deals with the optimization of a better form of a submarine (UV-LAHN) using a hydrodynamic performance analysis obtained from a digital investigation.

In this context, this study is divided into two part as follows:

1- Model calibration for submarine, mesh and boundaries conditions adaptation

2- Shape optimization, comparison and the choosing of the best form according to the drag

coefficient. Whereas, the hydrodynamics performances ( $Cd$ ,  $\lambda_{11}, \lambda_{22}, \lambda_{26}$ , and damping force) of optimum UV were analyzed

According to the drag force results comparison for many velocities, a good agreement was noted for the drag forces. The CFD can predict the hydrodynamics forces for submarine vehicles. However, the CFD optimization part of this paper revealed that  $n = 2$  and  $\alpha = 20$  was the optimal shape (UV-LAHN) by the confrontation of  $Cd$  for the eight submarines geometries;

The numerical investigation on the UV-LAHN showed that the added masses values is a smaller order for the velocities tested, which explains the low value of the drag force, in addition, the damping force linearity indicate that the optimal submarine UV-LAHN has a good hydrodynamics form.

## References

- [1] M. Karim, Numerical Computation of Viscous Drag for Axisymmetric Underwater Vehicles, *Journal Mekanikal*. Vol. 26, n. 2, 2008, pp.9 – 21.
- [2] X. Li, M. Zhao, FM. Zhao, QQ. Yuan, T. Ge, Study on hydrodynamic performance of Heavier-than-water AUV with overlapping grid method, *Ocean Syst Eng*. Vol. 4, n. 1, 2014, pp.1–19.
- [3] KM. Tan, T. Lu, F. Tien, A. Anvar, Drag coefficient estimation model to simulate dynamic control of autonomous underwater vehicle (AUV) motion, *20th International Congress on Modelling and Simulation*, 2013, pp. 1–6.
- [4] L. Wu, Y. Li, S. Su, p. Yan, Y. Qin, Hydrodynamic analysis of AUV underwater docking with a cone shaped dock under ocean currents, *Ocean engineering*. Vol. 85, 2014, pp. 110–126.
- [5] MSM. Aras, HA. Kasdirin, MH. Jamaluddin, MF. Basar, *of Engineering and Technology, Pro. Malaysian Technical Universities Conference*, Design and Development of an Autonomous Underwater Vehicle (AUV-FKEUTeM), Malaysia, 2009, pp. 1–5.
- [6] A. Saeidinezhad, AA. Dehghan, MD. Manshadi, Experimental investigation of hydrodynamic characteristics of a submersible vehicle model with a non-axisymmetric nose in pitch maneuver, *Ocean engineering*. Vol. 100, 2015, pp.26–34.
- [7] AD. Madan, MT. Issac, Hydrodynamic Analysis of AUV Hulls Using Semi-empirical

- and CFD Approach, *Universal Journal of Mechanical Engineering*. Vol. 5, n. 5, 2017, pp. 137–143.
- [8] A. Mitra, JP. Panda, HV. Warrior, The effects of free stream turbulence on the hydrodynamic characteristics of an AUV hull form, *Ocean Engineering*. Vol. 174, 2019, pp.148–158.
- [9] A. Phillips, M. Furlong, SR. Turnock, of *Ocean Engineering*, Pro. Oceans 2007, The use of computational fluid dynamics to assess the hull resistance of concept autonomous underwater vehicles, Europe, 2007, pp. 1–6.
- [10] P.Rattanasiri, PA.Wilson, AB.Phillips, Numerical investigation of a pair of self-propelled AUVs operating in tandem. Vol. 100, 2015, pp.126–137.
- [11] Y. Wang, T. Gao, Y. Pang, Y. Tang, Investigation and optimization of appendage influence on the hydrodynamic performance of AUVs, *Journal of Marine Science and Technology*. Vol. 24, n. 1, pp.297–305, 2019.
- [12] NM. Nouri, K. Mostafapour, SH. Hassanpour, CFD Modeling of Wing and Body of an AUV for Estimation of Hydrodynamic Coefficients, *Journal of Applied Fluid Mechanics*. Vol. 9, n. 6, 2016, pp.2717–2729.
- [13] V. Mishra, S. Vengadesan, SK. Bhattacharyya, Translational added mass of axisymmetric underwater vehicles with forward speed using computational fluid dynamics, *Journal of Ship Research*. Vol. 55, n. 3, 2011, pp.185–195.
- [14] T. Gao, Y. Wang, Y. Pang, J. Cao, Hull shape optimization for autonomous underwater vehicles using CFD, *Engineering applications of computational fluid mechanics*. Vol. 20, n. 1, 2016, pp.599–607.
- [15] DF. Myring, A theoretical study of body drag in subcritical axisymmetric flow, *The Aeronautical Quarterly*. Vol. 27, n. 3, 1976, pp.186–194.
- [16] P. Jagadeesh, K. Murali, Application of low-Re turbulence models for flow simulations past underwater vehicle hull forms, *Journal of Naval Architecture and Marine Engineering*. Vol. 2, n. 1, 2005, pp.41–54.
- [17] P. Jagadeesh, K. Murali, CG. Idichandy, Experimental investigation of hydrodynamic force coefficients over AUV hull form, *Ocean engineering*. Vol. 36, n. 1, 2009, pp.113–118.
- [18] Z. Nemouchi, Contribution à l'Etude des Jets Impactant Turbulents Présentant une Courbure des Lignes de Courant plus ou moins Faible, *Phd thesis*, Mentouri Constantine university, Algeria, 2012.
- [19] NM. White, A comparison between a simple drag formula and experimental drag data for bodies of revolution, *David W Taylor Naval Ship Research and Development Center Bethesda MD*. 1977.
- [20] C. Baker, Estimating drag forces on submarine hulls, *Defence R&D Canada – Atlantic, Report, DRDC Atlantic CR*, 2004.
- [21] C. Chin, M. Lau, Modeling and testing of hydrodynamic damping model for a complex-shaped remotely-operated vehicle for control, *Journal of Marine Science and Application*. Vol. 11, n. 2, 2012, pp.150–163.